



Fabrication of microchannels in single crystal diamond for microfluidic systems

Jiao Fu¹ · Zongchen Liu¹ · Tianfei Zhu¹ · Minghui Zhang¹ · Xiaofan Zhang¹ · Guoqing Shao¹ · Zhangcheng Liu¹ · Yanfeng Wang¹ · Dan Zhao¹ · Xiaohui Chang¹ · Yan Liang¹ · Juan Wang¹ · Jingwen Zhang¹ · Hong-Xing Wang¹

Received: 29 May 2018 / Accepted: 9 August 2018 / Published online: 14 August 2018
© Springer-Verlag GmbH Germany, part of Springer Nature 2018

Abstract

A growth of single crystal diamond (SCD) microchannels on HPHT diamond substrate has been carried out successfully by a simple and novel method. Firstly, aluminum film was patterned on SCD diamond substrate surface by magnetron sputtering, photolithography and dry etching techniques. Secondly, the aluminum patterns were transferred onto diamond substrate via inductively coupled plasma etching to form grooves on diamond surface. Finally, microchannels were achieved by epitaxial lateral overgrowth of SCD on the surface of prepared substrate by microwave plasma chemical vapor deposition system. After that, fluorescent liquid was introduced to check hollowness of the microchannels. This work provides a simple and time saving method to fabricate SCD microchannels for microfluidic system, which offers a great potential for hard environment applications.

Keywords Single crystal diamond · Epitaxial lateral overgrowth · Microchannels · Microfluidic systems

1 Introduction

Compared with traditional microchannel materials, diamond is an excellent material due to its extremely properties such as highest thermal conductivity, low friction coefficient, high mechanical hardness, chemical inertness, high breakdown voltage, high electrical resistance, low dielectric constant as well as outstanding biocompatibility (May 2008; Gaidarzhly et al. 2007). The employment of diamond would present a significant improvement in hard environment applications. For example, it is a material of heat spreader channel system in high-temperature chemical reactions to high power electronic devices as a result of its highest thermal conductivity (Asmussen and Reinhard 2002). It is also a biosensing material for drug transport on account of its biocompatibility as well as high-chemical stability and largest optical bandgap (Kim et al. 2007). Moreover, it owns substantial benefits of electroosmotic pumping systems with highly corrosive fluids due to its excellent thermal, chemical, mechanical and semiconductor properties (Becker and Locascio 2002).

Nevertheless, diamond is difficult to be micromachined due to its mechanical hardness and chemical stability and also be lacking of well-established diamond micromachining technique. Previously, due to the difficulty of forming heteroepitaxial single crystal diamond films, diamond microchannels were mainly fabricated on polycrystalline films via sacrificial layer technology (Chandran et al. 2017; Muller et al. 2004, 2005). Compared to SCD, polycrystalline diamond has disadvantages of grain boundaries, impurities, relatively high friction coefficient and large stress of films (Guillen et al. 2005), which cause degradation of performance and poor reproducibility. Recently, researchers focus on finding feasible ways to fabricate SCD microchannel using laser machining (Jedrkiewicz et al. 2017; Su et al. 2013), ion beam lithography (Picollo et al. 2017; Strack et al. 2013) and epitaxial lateral overgrowth (Fu et al. 2017) techniques. This paper reports a simple and time saving way to fabricate a batch of SCD microchannel structures on HPHT diamond substrate via etching groove and ELO growth techniques. It is a significant development towards fabrication of microchannel with theoretically excellent material for microfluidic system.

✉ Hong-Xing Wang
hxwangcn@mail.xjtu.edu.cn

¹ Institute of Wide Band Gap Semiconductors, Xi'an Jiaotong University, Xi'an, China

2 Experiment details

The HPHT Ib (001) SCD substrate was used in this experiment. Aluminum film with thickness of 6 μm was deposited on the surface of substrate by magnetron sputtering method. The SPR220 photoresist (PR) was spun on diamond substrate with a speed of 5000 rpm, resulting a PR thickness of about 6 μm . Then the standard photolithography process was used to form PR stripes with width of 30 μm and the distance between two stripes was 30 μm . After patterning, the PR stripes were transferred onto aluminum surface by inductively coupled plasma (ICP) etch process until all unmasked aluminum was etched out, during which Cl_2 , BCl_3 and Ar were used as etching gases. Then, grooves were processed in the area without aluminum covered areas by ICP etching, during which O_2 and Ar were used as the reaction gases with the flow rates of 50 and 20 sccm, respectively. After etching, the thickness of aluminum stripes decreased to approximately 500 nm. The sample was ultrasonically cleaned by a HCl solution to lift-off aluminum stripes. Then, SCD microchannels were fabricated by loading the patterned groove sample into MPCVD chamber for ELO growth until the growth sidewalls were connected continuously. The thickness of the as-grown diamond layer was about 100 μm . The microchannel fabrication processes are schematically illustrated in Fig. 1.

3 Results and discussion

The morphologies of fabricated SCD grooves were characterized by optical microscope (OM), scanning electron microscopy (SEM), and laser scanning confocal microscopy (LSCM), as shown in Fig. 2. Figure 2a, b are the OM and SEM images, indicating a bright strip of diamond windows with a relative smooth surface and a clear boundary, and a dark strip of fabricated grooves. Figure 2c, d shows the typical LSCM image and the cross sectional profiles of the fabricated SCD grooves, exhibiting that the width and depth of each groove is about 30 and 20 μm , the distance between two adjacent grooves is about 30 μm and the grooves sidewall have an inclination between 2° and 6° from vertical by ICP etching. Additionally, the profile indicates that the bottom roughness is about 8 nm.

Figure 3a is a SEM image of the sample surface after 5 h growth by MPCVD, illustrating that diamond grooves have been covered completely during ELO growth. The as-grown sample surface morphology was measured by AFM within the area of $100 \times 100 \mu\text{m}^2$, indicating a smooth surface with a roughness of 10 nm, as shown in

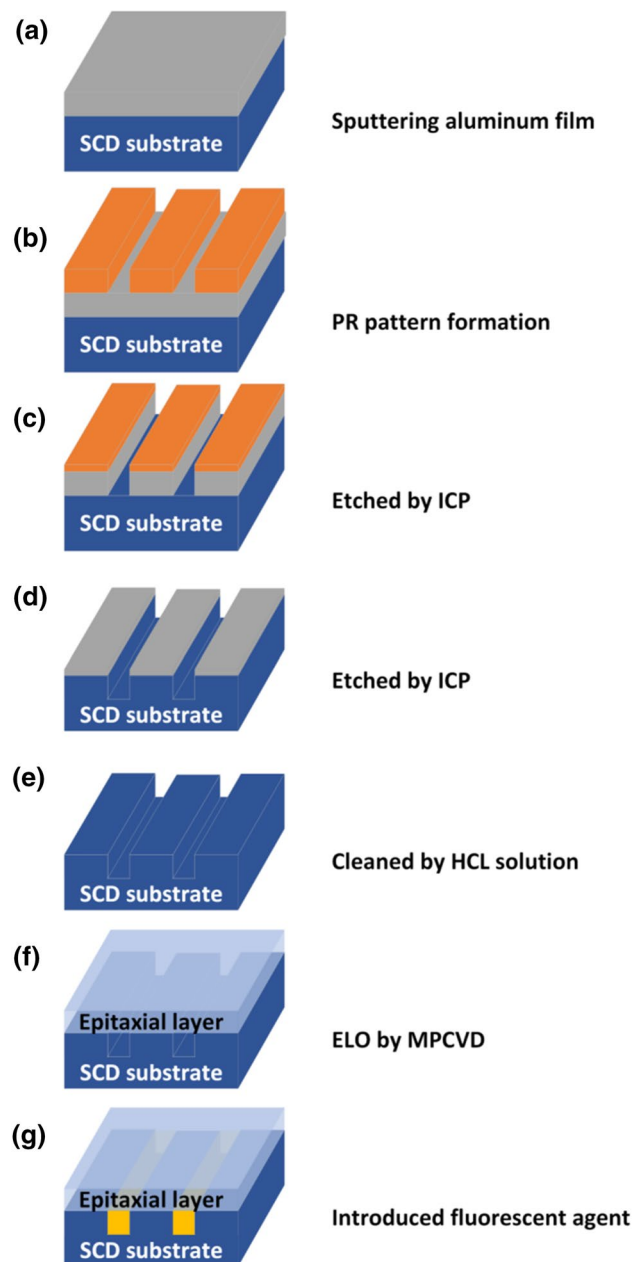


Fig. 1 Schematic of SCD microchannel fabrication process

Fig. 3b. Figure 3c is the optical microscope image taken with both reflection and transmission light. The hazily bright and dark strips are corresponding to diamond window and groove area, indicating a microchannel with neat edge. The groove area is darker than diamond window area because the light was reflected to the other direction by the microchannel sidewalls.

The cross section of the microchannels and its enlarged view are shown in Fig. 4a, b, respectively. The length and height of the fabricated microchannels were measured to be 2.35 and 21.35 μm , respectively. Figure 4c shows the Raman

Fig. 2 SCD substrate after ICP etching **a** OM image, **b** SEM image (tilt 45°), **c** LSCM image, **d** cross section profile obtained by LSCM

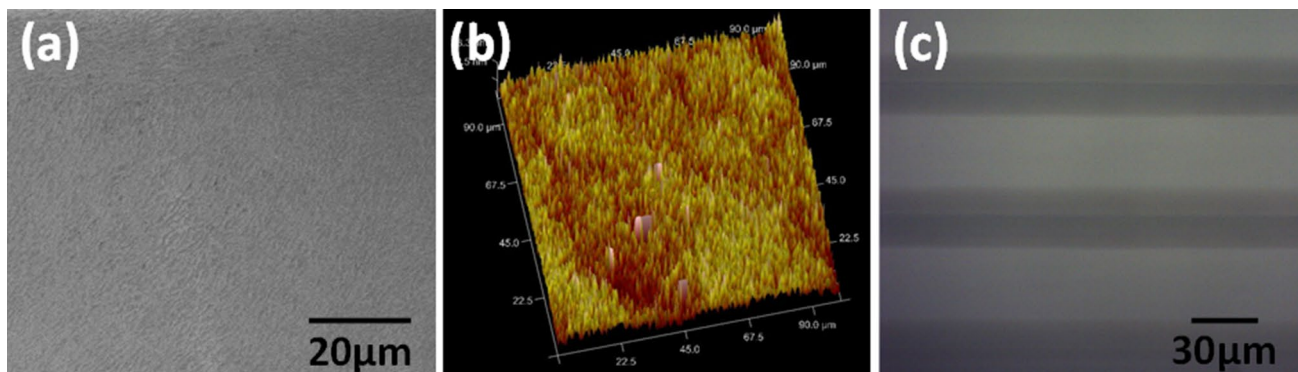
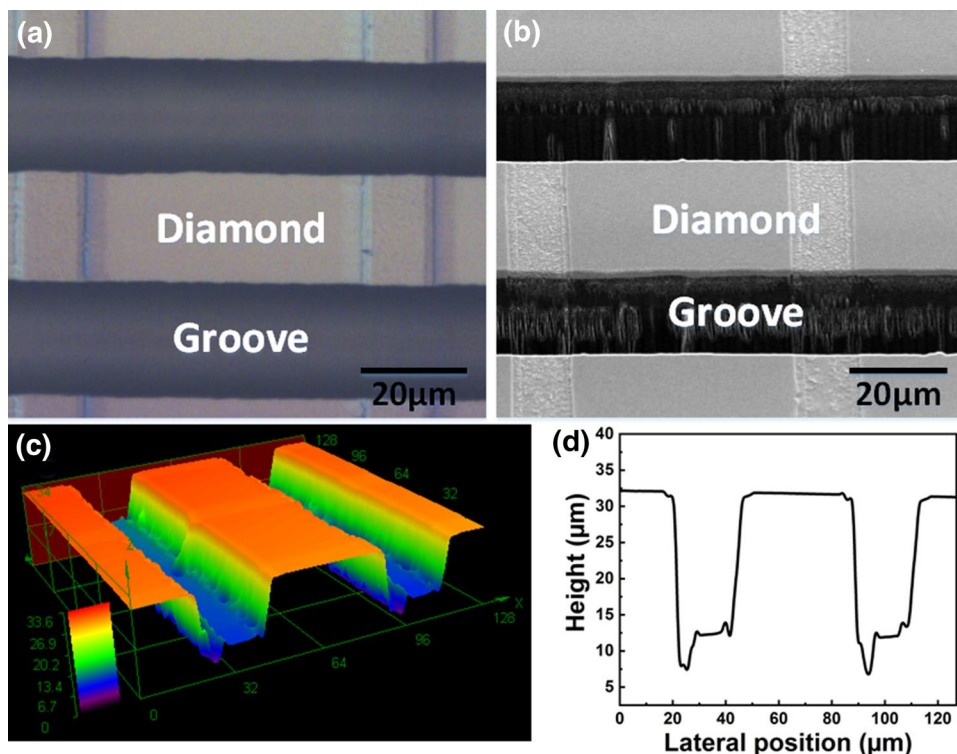


Fig. 3 SCD microchannel sample after 5 h ELO growth. **a** SEM image, **b** AFM image, **c** optical image focusing on microchannels

spectra of points I–VI indicated in Fig. 4a, whose Raman excitation wavelength was 532 nm. There is a sharp peak shown in microchannel measurement at 1333 cm^{-1} , revealing good composition of diamond sp^3 (Steven and Robert 2004). Meanwhile, full widths at half maximum (FWHM) of diamond Raman spectra (points I–V) are approaching to that of substrate (point VI), and peaks located at $1400\text{--}1450\text{ cm}^{-1}$ appear in Raman spectra are typical peaks related to the fluorescence of CVD grown diamond with N_2 introduction.

To evaluate the quality of ELO film, XRD investigation has been carried out as shown in Fig. 5b. For comparison, the quality of substrate has also been checked whose result

are presented in Fig. 5a. The FWHM values of the substrate and ELO film are 0.01031° and 0.03878° , respectively, indicating an acceptable quality of ELO diamond film compared with that of the substrate (Wang et al. 2016; Yan et al. 2002).

Then, sample with microchannels was immersed into fluorescent liquid to check the continuity. Figure 6a shows a schematic of fluorescent liquid in microfluidic channels. A Nikon A1 laser scanning confocal microscopy was performed to detect the number of photons to check the presence of liquid inside of fabricated channels. As the channel structure of the diamond sample hosts nitrogen-vacancy (NV) fluorescent complexes in high concentrations at 575 and 637 nm, it was necessary to choose a fluorophore

Fig. 4 **a** Cross section SEM images of the SCD microchannels. **b** Enlarged view of **a**. **c** Raman spectra taken from different locations around the channel (as shown in the adjacent SEM images)

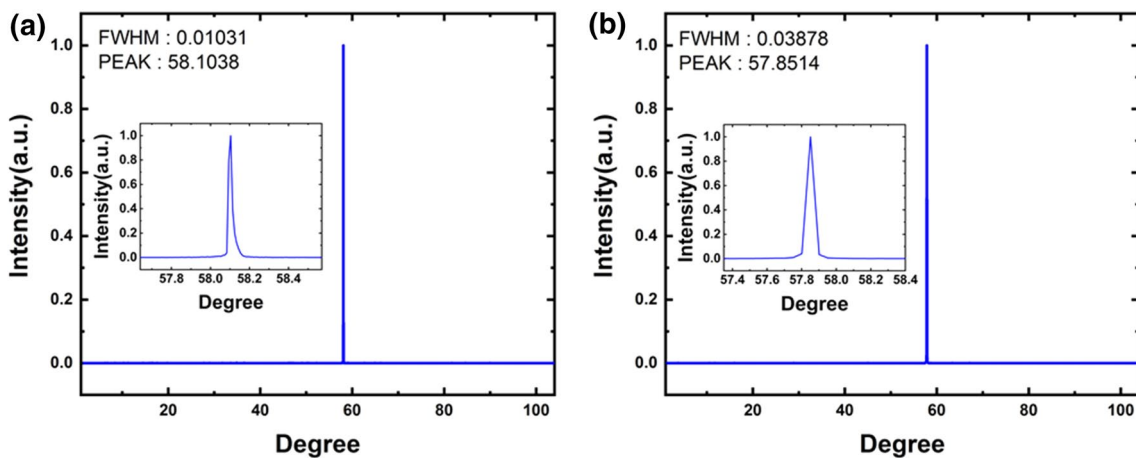
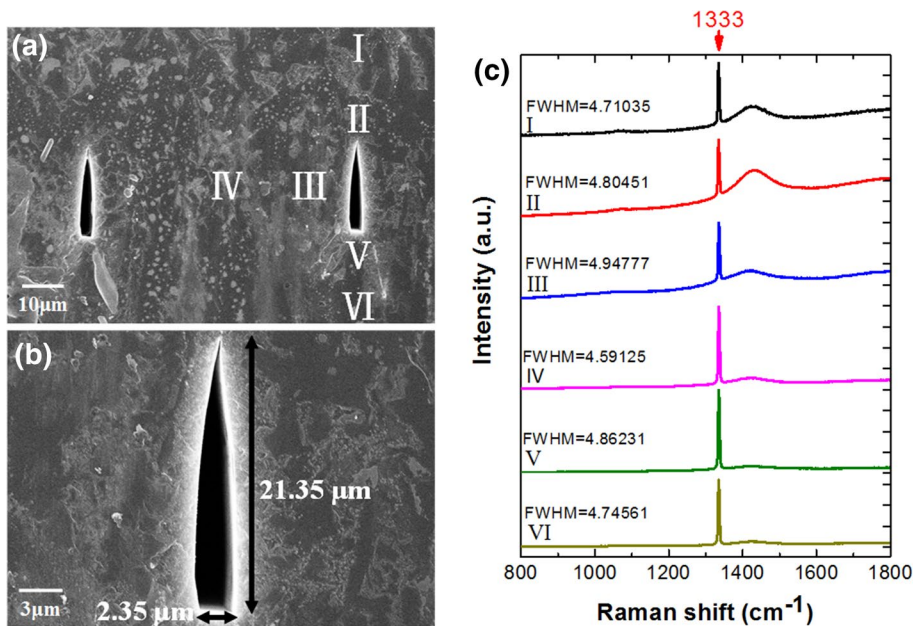


Fig. 5 XRD spectra **a** substrate. **b** As grown diamond film

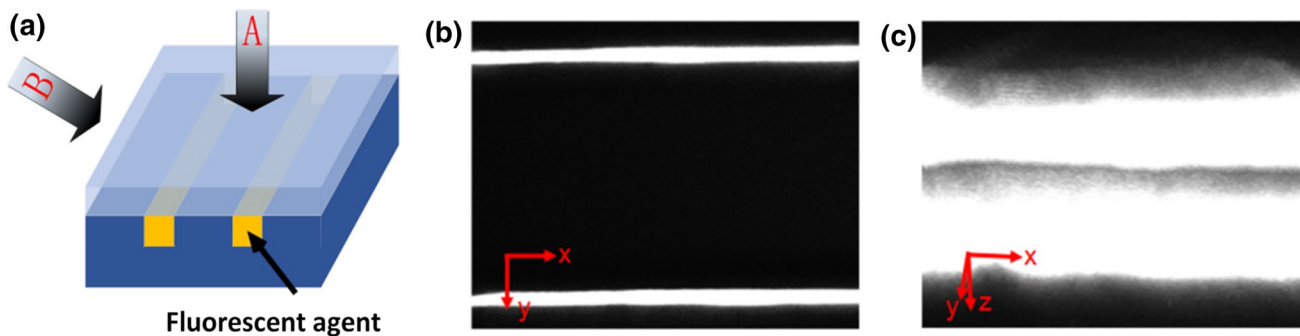


Fig. 6 **a** Schematic of SCD microchannel with fluorescent liquid. Laser scanning confocal microscope images of **b** two-dimensional diagram corresponding to “A” direction in **a**. **c** Three-dimensional diagram corresponding to “B” direction in **a**

whose emission features do not overlap with that of the NV center of diamond. Fluorescent liquid with emission peak at 480 nm was used in our experiment. Confocal microscope image taken from directions “A” and “B” is shown in Fig. 6b, c, respectively. The excitation and detector wavelengths are 408 and 425–550 nm, respectively. An intense and uninterrupted luminescence were observed, indicating that microchannels were hollow and continuous.

4 Conclusions

In summary, we report a simple method to fabricate SCD microchannel structure on diamond substrate by etching groove and ELO growth technology. Raman and XRD spectra were used to evaluate the diamond film in microchannel areas, indicating an acceptable quality. The intense and uninterrupted luminescence confocal microscope images taken from ELO diamond sample indicate that the microchannel are hollowness and continuity. The processes in this work may provide a feasible method to fabricate SCD microchannel for microfluidic systems which can be applicable in hard environment.

Acknowledgements This work was supported by the Science and Technology Coordinating Innovative Engineering Projects of Shaanxi Province (Grant no. 2016KTZDGY02-03). The SEM work was done at International Center for Dielectric Research (ICDR), Xi’an Jiaotong University, Xi’an, China, we thank to Ms. Dai for her help in using SEM; The LSCM work was done at The State Key Laboratory for Manufacturing Systems Engineering, Xi’an Jiaotong University, Xi’an, China, we thank to Ms. Qu for her help in using LSCM.

References

- Asmussen J, Reinhard D (2002) *Diamond films handbook*. CRC, Boca Raton
- Becker H, Locascio LE (2002) Polymer microfluidic devices. *Talanta* 56:267
- Chandran M, Elfimchev S, Michaelson S, Akhvediani R, Ternyak O, Hoffman A (2017) Fabrication of microchannels in polycrystalline diamond using pre-fabricated Si substrates. *J Appl Phys* 122:145303
- Fu J, Zhu TF, Zhang MH, Zhang X, Li FN, Liu ZC, Denu GA, Wang YF, Zhao D, Shao GQ, Chang XH, Wang W, Zhang JW, Wang HX, Wang JJ, Hou X (2017) Fabrication of single crystal diamond microchannels for microelectromechanical systems. *Diam Relat Mater* 80:64
- Gaidarzhy A, Imboden M, Mohanty P, Rankin J, Sheldon BW (2007) High quality factor gigahertz frequencies in nanomechanical diamond resonators. *Appl Phys Lett* 91:203503
- Guillen FJH, Janischowsky K, Kusterer J, Ebert W, Kohn E (2005) Mechanical characterization and stress engineering of nanocrystalline diamonds films for MEMS applications. *Diam Relat Mater* 14:411
- Jedrkiewicz O, Kumar S, Sotillo B, Bollani M, Chiappini A, Ferrari M, Ramponi R, Trapani PD, Eaton SM (2017) Pulsed Bessel beam-induced microchannels on a diamond surface for versatile microfluidic and sensing applications. *Opt Mater Express* 7:1962
- Kim L, Toh YC, Voldman J, Yu H (2007) A practical guide to microfluidic perfusion culture of adherent mammalian cells. *Lab Chip* 7:681
- May PW (2008) The new diamond age? *Science* 319:1490
- Muller R, Schmid P, Munding A, Gronmaier R, Kohn E (2004) Elements for surface microfluidics in diamond. *Diam Relat Mater* 13:780
- Muller R, Gronmaier R, Janischowsky K, Kusterer J, Kohn E (2005) An “all-diamond” inkjet realized in sacrificial layer technology. *Diam Relat Mater* 14:504
- Piccolo F, Battiato A, Boarino L, Tchernij SD, Enrico E, Forneris J, Gilardino A, Jakšić M, Sardi F, Skukan N, Tengattini A, Olivero P, Re A, Vittone E (2017) Fabrication of monolithic microfluidic channels in diamond with ion beam lithography. *Nuclear Instrum Methods Phys Res B* 404:193
- Steven P, Robert JN (2004) Raman spectroscopy of diamond and doped diamond. *Phil Trans R Soc Lond A* 362:2537
- Strack MA, Fairchild BA, Alves ADC, Senn P, Gibson BC, Praver S, Greentree AD (2013) Buried picolitre fluidic channels in single-crystal diamond. *SPIE Proc* 8923:89232X
- Su S, Li J, Lee GCB, Sugden K, Webb D, Ye H (2013) Femtosecond laser-induced microstructures on diamond for microfluidic sensing device applications. *Appl Phys Lett* 103:231913
- Wang F, Shan C, Yan J, Fu J, Abdisa DG, Zhu T, Wang W, Chen F, Zhang J, Wang HX, Hou X (2016) Application of femtosecond laser technique in single crystal diamond film separation. *Diam Relat Mater* 63:69
- Yan C, Vohra YK, Mao H, Hemley RJ (2002) Very high growth rate chemical vapor deposition of single-crystal diamond. *Proc Natl Acad Sci USA* 99(20):12523

Publisher’s Note Springer Nature remains neutral with regard to jurisdictional claims in published maps and institutional affiliations.